ACS APPLIED MATERIALS & INTERFACES

Research Article

www.acsami.org

Colorimetric Determination of DNA Methylation Based on the Strength of the Hydrophobic Interactions between DNA and Gold Nanoparticles

Yi-Zhen Lin and Po-Ling Chang*

Department of Chemistry, Tunghai University, Taichung 40704, Taiwan

Supporting Information

ABSTRACT: A simple, novel colorimetric nanosensor for DNA methylation based on the strength of hydrophobic interaction between DNA and gold nanoparticles was proposed. The nanosensing of oligonucleotides with four nitrogen bases was first demonstrated by dividing the bases into two groups (A/T and C/G) using the representative colors that correspond to Watson−Crick base pairing. By treatment of the genomic DNA with sodium bisulfite followed by PCR amplification, the methylation level of nasopharyngeal carcinoma cells treated with 5-aza-2′-deoxycytidine for up to 5 days could be discriminated by naked eye observation. Furthermore, 12 cancer cell lines that demonstrate heterogeneity with respect to DNA methylation could also be distinguished using the nanosensor, even for amplicons as long as 342 bp. These results demonstrate that the proposed colorimetric nanosensor could potentially be useful in epigenetic studies.

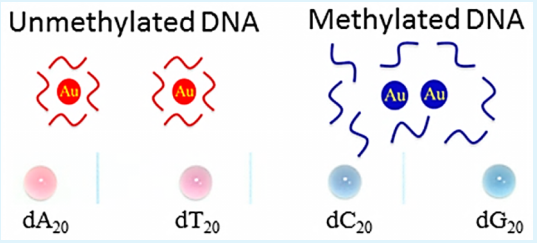

KEYWORDS: *cancer, DNA methylation, epigenetics, nanoparticles, sensor*

INTRODUCTION

DNA methylation plays an important role in gene expression due to the inhibition of the transcription of down-regulated genes.[1] To date, DNA methylation has been demonstrated with respect to embryonic development,[2] cancer growth,[3,4] aging,[5] and in cancer therapy.[6] Moreover, DNA methylation can reportedly serve as a biomarker for early disease diagnosis.[7] However, the determination of DNA methylation typically relies on specialized instruments such as capillary electrophoresis,[8,9] methylation sensitive high-resolution melting (MS-HRM) analysis,[10,11] and next-generation sequencing.[12,13] For example, Schmitz et al. used capillary electrophoresis to determine the total 5-methylcytosine (^{5m}C) content within the entire genome.[14] This technique is simple, but the methylation level for a specific DNA region cannot be obtained because the genomic DNA must be fully digested into deoxynucleotide monophosphate. The determination of global genomic DNA methylation could also be accomplished by fluorescence polarization, combined capillary electrophoresis immunoassay,[15] and ultrahigh performance liquid chromatography/tandem mass spectrometry.[16] To determine the DNA methylation aimed at a specific gene, combined bisulfite restriction analysis (COBRA) is useful for exploring the DNA methylation of PCR amplicons.[17] Combining COBRA and capillary electrophoresis was also useful for quantitation of DNA methylation[8] and for the determination of the heterogeneity of DNA methylation.[9] However, the use of COBRA to evaluate a methylation level restricts the focus to a few CpG sites among the amplicons due to the limited availability of the endonuclease. A real-time PCR-based method called MS-HRM was developed by Wojdacz et al.[10] A reasonable amplicon size and sensitive saturation dye[18] are typically required to build a successful MS-HRM.[11] Methylation pyrosequencing is considered the gold-standard method for determining DNA methylation because it can precisely read each CpG dinucleotide.[12] However, these aforementioned methods require special and/or expensive instruments to obtain reliable data.

In recent years, colorimetric nanosensors have become popular because they provide several practical advantages, including the ability for naked-eye visualization, cost effectiveness, simplicity, portability and a low detection limit.[19,20] Elghanian et al. first reported the determination of an oligonucleotide by observing the optical properties of gold nanoparticles (AuNPs) using the naked eye.[21] Huang et al. presented a fluorescent gold nanosensor for the sensitive determination of mercury ions.[22] In another study, Li et al. used the concept of T−Hg^{II}−T[23] to determine the mercury ion content based on a nanometal surface energy transfer.[24] Ferhan et al. also proposed a solid-phase colorimetric sensor for the determination of lead ion based on the AuNPs-loaded polymer brushes.[25] In addition to the metal ion, Liu et al. also reported a simple method for the selective and sensitive detection of endogenous biological cyanide and cyanogenic glycoside using polysorbate 40-stabilized AuNPs.[26] Furthermore, Wang et al. reported a novel assay for the determination of ATP by

Received: September 7, 2013
Accepted: November 7, 2013
Published: November 7, 2013

unmodified AuNPs.[27] Li and colleagues also used the unmodified AuNPs to investigate the interaction of amino acids,[28] to assay protein poly(ADP-ribosyl)ation[29] and to determine the single-nucleotide polymorphism of triplex DNA.[30] Moreover, Liu et al. reported a novel method to determine the activity of DNA methyltransferase using DNA modified AuNPs coupled with an enzyme-linkage reaction of DNA adenine methyltransferase and a methylation sensitive restriction endonuclease.[31] Recently, Wang et al. announced a quartz crystal microbalance (QCM)-based assay for label-free detection of DNA methylation.[32] In this article, the genomic DNA was digested by the methylation sensitive restriction endonuclease (*Hpa*II) followed by PCR amplification. Finally, the amplicons were then measured by DNA probe-immobilized QCM based on the resonance frequency shift. In this article, we propose a novel colorimetric nanosensor for DNA methylation based on the strength of adsorption between DNA and AuNPs. Unlike the traditional nanosensor, surface modification of specific biomolecular ligands on the AuNPs is not required in the proposed method. In addition, our result also indicates that the different strength of DNA adsorption on AuNPs is sufficient to discriminate the nitrogen base of DNA, which allows the methylation states of a specific CpG island to be determined for a cancer cell's microRNA gene.

MATERIALS AND METHODS

Synthesis of Gold Nanoparticles. The synthesis of 13 nm AuNPs was modified slightly from that presented in the literature.[33] A 1 mL sample of sodium tetrachloroaurate(III) dehydrate (Sigma-Aldrich) (250 mM) was dissolved in 249 mL of double-deionized water (ddH_2O, >18 MΩ) in a three-necked flask and heated on a hotplate until boiling, followed by 5 min of stirring. A certain quantity of sodium citrate was then added to yield a final concentration of 3.88 mM. The reaction was heated for an additional 15 min, at which time the solution's color changed from yellow to dark red. Finally, the heated three-necked flask was carefully transferred to an ice bath for cooling. The as-synthesized wind-red AuNPs (maximum absorbance at 518 nm) were transferred to a glass-bottomed container, and mercaptopropionic acid (MPA) (Sigma-Aldrich) (1 mM, 500 μL) was added for surface modification of the carboxylic groups on the AuNPs. The mixture was stirred overnight and stored at 4 °C. Prior to nanosensing of the DNA methylation, 1 mL of the well-prepared AuNPs (1×) was transferred to a 1.5 mL plastic vial and centrifuged at 10000*g* for 30 min to remove any excess MPA. The modification with the MPA increased the stability of the AuNPs with repeated washing with double-deionized water. The MPA-capped AuNPs did not change color with the tested oligonucleotide and only showed a slight increase in the resistance to the salt-induced aggregation when compared to that of the naked AuNPs (Figure S1, Supporting Information). The gold pellet was then resuspended in 500 μL (the AuNPs were concentrated 2-fold) of ddH_2O and ready for nanosensing.

Cell Culture, Bisulfite Conversion, Nested PCR, and Real-Time PCR. Lung cancer (NCIH1299), NPC (TW02, TW04), breast cancer (MCF7), oral cancer (OECM-1), liver cancer (J7), and cervical cancer (HeLa) cell lines were kindly provided by the Molecular Medicine Research Center of Chang Gung University. The NPC cells (HK-1) and the EBV-positive NPC cells (C666-1) were kindly provided by Prof. Sai-Wah Tsao from the Department of Anatomy at the University of Hong Kong. The cells were cultured in Roswell Park Memorial Institute RPMI medium (RPMI-1640) at 37 °C in 5% CO_2 for 3 days. For the demethylation of DNA, the HK-1 cells were treated with 5-aza-2′-deoxycytidine (Sigma Aldrich) for 1, 3, 4, and 5 days. Briefly, the HK-1 cells were incubated in a culture medium that contained 5-aza-2′-deoxycytidine (10 μM) for the desired days with the culture medium being replaced every day with fresh medium containing 5-aza-2′-deoxycytidine. All DNAs were extracted from the cell lines using a commercial reagent according to the manufacturer's instructions (Qiagen). DNase/RNase-free water was used to adjust the concentration of the synthetic oligonucleotides, and all DNA samples were stored at −20 °C. The extracted DNA samples were treated with a bisulfite reagent according to the literature.[34] A 1 μg sample of genomic DNA (20 μL) was added to a microtube containing 130 μL of CT conversion reagent. After the solution was briefly mixed, the tube was placed on a PCR thermalcycler (Astec) for incubation at 98 °C for 10 min, at 65 °C for 2.5 h, and at 4 °C for 20 h. The mixture was then transferred to a Zymo-Spin IC Column containing 600 μL of M-binding buffer and was centrifuged at 10000*g* for 30 s. After another wash with 200 μL of M-wash buffer, 200 μL of M-desulfonation buffer was added to the collection tube, which was incubated at ambient temperature for 20 min. The collection tube was then washed twice with 200 μL of of M-wash buffer (10000*g*, 30 s). Finally, the microtube was transferred to a new 1.5 mL centrifuge tube, and the genomic DNA was eluted with ddH_2O via centrifugation (30 s at 10000*g*). Customized synthetic oligonucleotides including primer pairs for PCR were purchased from Integrated DNA Technologies. The 3D structure of oligonucleotides was calculated and drawn using MarvinSketch (ChemAxon).

The *Homo sapiens* microRNA 9-1 (NCBI Reference Sequence: NR_029691.1) was used as the target gene in this study. The CpG islands of microRNA 9-1 were predicted by searching the partial sequence of the q-arm of chromosome 1 (band: 1q22, Chr1: 156390154-156391831) obtained from USCS.[35] The original sequence was then converted to a new bisulfite-converted sequence by Methyl Primer Express (Applied Biosystems), and the sequence was used to design the primer for PCR amplification. For the nested PCR, the following external primers were designed for the first amplification: miR9-1F (gagattatttagggttgtgaaaatg) and miR9-1R (aaaaactaaaaatcaacacaaaaac). The 25 μL PCR mixtures contained 2.5 μL of 10× PCR buffer, 0.5 μL of primers (10 μM), 2 μL of dNTPs (2.5 mM), 2.0 units of FastStart *Taq* DNA polymerase (Roche), and 1 μL of the DNA template with double-deionized H_2O to yield a final volume of 25 μL. Following 30 amplification cycles (30 s at 95 °C, 30 s at 50 °C, 60 s at 72 °C), 1 μL of the initial amplified products (638 bp) was transferred to another microtube that contained a new PCR mixture and the internal primers (miR9-1-1F: ggattagagattatttagggttgtgaa and miR9-1-1R: taaaaacaaaacaacctcctctacc) for the second PCR amplification. The thermocycler was programmed for denaturation for 4 min at 95 °C followed by 35 amplification cycles (30 s at 95 °C, 30 s at 55 °C, 30 s at 72 °C) and an extra elongation step for 7 min at 72 °C. The nested PCR products for the miR9-1 were 342 bp long.[34] The reaction mixtures were then washed using a silica-membrane-based PCR cleanup kit (Geneaid) to remove the salt, dNTPs, and primers. Finally, the concentrations of the cleaned PCR products were obtained using an absorption spectrophotometer (Shimadzu). The real-time PCR were performed by an Eco Real-Time PCR System (Illumina, CA, USA) with a hold at each step on the SYBR channel. The fluorescence of the high-resolution melting curve was monitored from 60 to 95 °C in 1 °C increments. The components and temperature setting of real-time PCR was the same as described above except to the saturating dye-SYTO9[36] (final concentration: 5 μM for each reaction mixture). The MS-HRM data were then exported and replotted by Origin version 7 (OriginLab, MA, USA).

Determination of DNA Methylation by Nanosensing. The synthetic oligonucleotide (Integrated DNA Technologies) sample (1 μM, 1 μL) or PCR amplicons (50 ng) and 5 μL of AuNPs were transferred into a plastic microtube and adjusted to a final volume of 10 μL with double-deionized H_2O. The mixture was heated at 94 °C (30 s) for DNA denaturation followed by cooling to 25 °C for 30 s. One microliter of Tris-acetate buffer (pH 8.0, 40 mM) was then added to the sample mixture, which was allowed to stand for 5 min at room temperature to destabilize the AuNPs. Finally, 1 μL of $NaClO_4$ (100 mM) was added into the microtube and the solution was allowed to sit for another 5 min. Once the nanosensing process was completed, the sample mixtures (10 μL) were transferred to a paraffin-covered paper box and photographed using a commercial digital camera (Canon 600D) without any image modification via software.

RESULTS AND DISCUSSION

Strategy of Nanosensing for DNA Methylation. To determine DNA methylation for a specific downstream gene using the proposed nanosensor, as shown in Scheme 1, a

Scheme 1. Schematic Diagram of the Nanosensing for DNA Methylation Workflow[a]

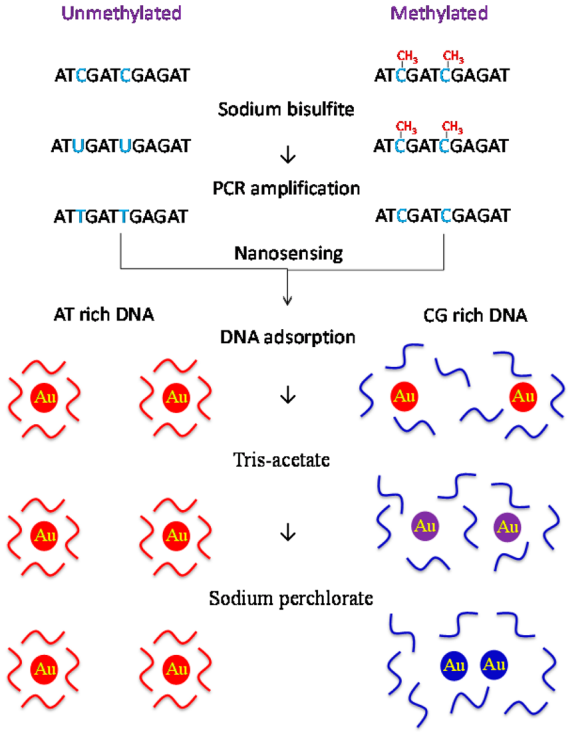

[a]The genomic DNA was treated with sodium bisulfite followed by PCR amplification. The AuNPs were mixed with the PCR amplicons, and the solution was heated to 94 °C for denaturation. After the DNA was denaturized and adsorbed onto the AuNPs, Tris-acetate (4 mM, pH 8.0) was added into the sample mixture to develop the color. For color enhancement, we added sodium perchlorate to the sample mixture to further destabilise the AuNPs. Finally, the colorful AuNPs were captured using a commercial digital camera. For the experimental details, please refer to the Results and Discussions.

bisulfite treatment of the genomic DNA is necessary to distinguish the methylated cytosine (^{5m}C) from unmethylated cytosine because the unmethylated cytosine can be converted to uracil.[17] Following PCR amplification, the methylated cytosine loses its methyl group, but the uracil (from the bisulfite conversion of unmethylated cytosine) can be converted to thymine during the PCR process according to the principle proposed by Clark et al. for bisulfite genomic sequencing.[37] The double-stranded PCR products are then mixed with AuNPs followed by a high temperature incubation to obtain the denatured single-stranded DNA. Once the temperature is decreased rapidly to ambient temperature, the adsorption of the single-stranded DNA on the AuNPs can be expected.[38] The nitrogen bases of the PCR products that represent the original methylation state are quite different from each other; therefore, the surface of the AuNPs should also represent a dissimilar status because of the strength and/or quantity of DNA adsorption. On the basis of the hypothesis, a salt-induced aggregation of AuNPs should be used to differentiate between AT-rich (unmethylated) or CG-rich (methylated) DNA protected AuNPs as a result of different DNA adsorption. The following question remains to be addressed: how can the nitrogen bases be differentiated by physical adsorption onto the AuNPs? Before nanosensing, a suitable "competent" buffer must be chosen as destabilized buffer as a result of the chosen buffer should not only cause the aggregate between AuNPs but also keeping the discriminatory ability for nitrogen base of DNA. As shown in Figure 1, various

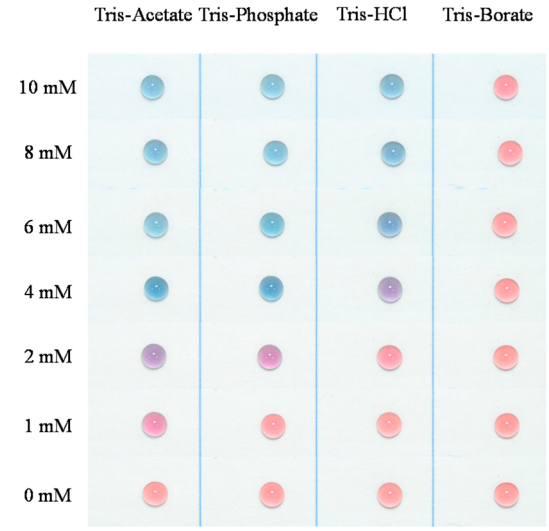

Figure 1. Effect of the buffers on AuNP aggregation. The buffers of various concentrations were directly mixed with the AuNPs to stabilize the AuNPs.

buffers were chosen to test the stability of AuNPs. Under pH 8.0, the Tris-borate buffer appeared more stable for AuNPs whereas the Tris-acetate (TA) made the AuNPs agglomerated, even the TA as low as 1 mM. Because the goal of this study is dependent on the DNA protection ability for AuNPs, the minimum buffer concentration that could induce the AuNP aggregation (Tris-acetate, 4 mM) was chosen. Each buffer was adjusted using a particular acid to pH 8.0 and then used as a destabilizing agent for AuNPs in following studies.

Discriminating Power of AuNPs for Oligonucleotides. In Figure 2, four oligonucleotides (dA_{20}, dT_{20}, dC_{20}, dG_{20}) were used to test the discrimination power of the AuNPs. The sample mixtures (AuNPs and DNA) were heated to 94 °C for 30 s to denature the DNA. Then, the temperature was decreased to ambient temperature, and the samples were allowed to stand for 30 s to allow the single-stranded DNA to adsorb onto the AuNPs. As shown in Figure 2a, the colors of the DNA adsorbed onto AuNPs remained consistent, as anticipated. However, when a destabilizing buffer, Tris-acetate (TA) (4 mM, pH 8.0) (Figure 1), was added into each mixture, the AuNPs aggregated. This critical step also induced changes in the color of the AuNPs with the different levels of aggregation (Figure 2b). The violet color of the dC_{20}-AuNPs and dG_{20}-AuNPs indicates that the AuNPs aggregated in the sample mixture to a greater extent than the dA_{20}-AuNPs and dT_{20}-AuNPs due to a surface plasmon resonance shift of the AuNPs.[21] To enhance the color range and improve the discrimination power of the AuNPs, $NaClO_4$ was added to the reaction mixtures to further destabilize the AuNPs according to a previous study by Li et al.[39] When the 10 mM (Figure 3) $NaClO_4$ was added into the mixture, the color could be divided

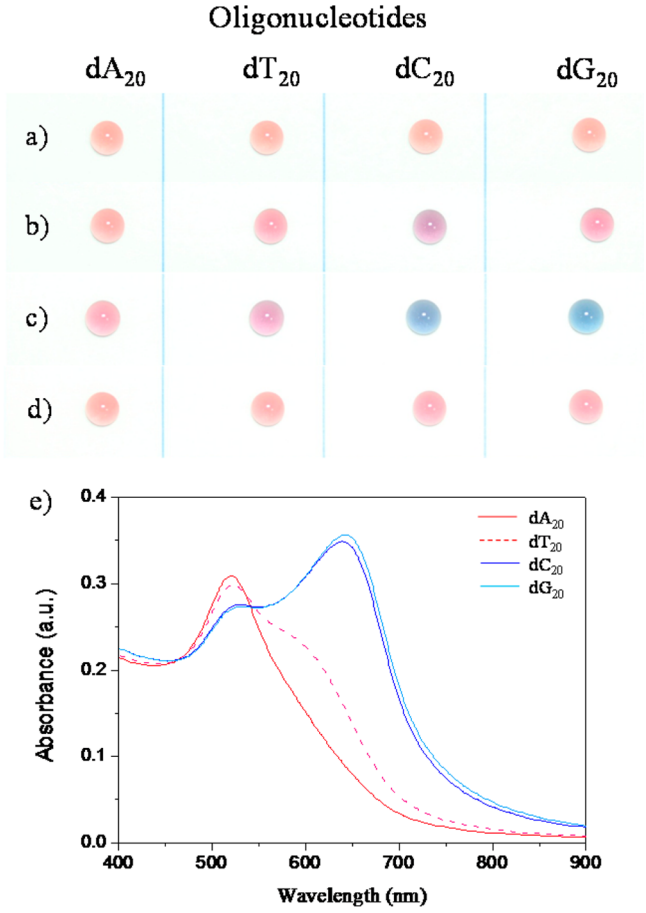

Figure 2. Discrimination power of the nanosensor for oligonucleotides. (a) The AuNPs (1×) were added to the DNA sample in a 1:1 ratio and heated at 94 °C for 30 s and then allowed to stand for 30 s at ambient temperature (25 °C). (b) The TA buffer (4 mM, pH 8.0) was added to the DNA-protected AuNPs. (c) The $NaClO_4$ (10 mM) was added to the aggregated AuNPs to enhance their color. (d) Only $NaClO_4$ (10 mM) was added to the DNA-protected AuNPs. (e) The absorption spectrum of c.

into two groups: A/T and C/G (Figure 2c). The results demonstrate the AuNPs are good enough to discriminate the nitrogen base of DNA. In contrast, as shown in Figure 2d, sodium perchlorate (10 mM) alone cannot induce the aggregation of the DNA-protected AuNPs. Because the many negative charges on the DNA backbone should be repulsed by citric acid and some $AuCl_2^-$ on the AuNPs[40] under low ionic-strength conditions, the AuNP protection by the DNA is governed by a physical interaction and not an electrostatic attraction. The interaction between the nitrogen bases and the gold is thought to be governed by van der Waals forces as well as the coordination between the lone electron pairs on atoms in the bases and the gold.[41] Previous research indicated that the longer DNA molecule could enhance the hydrophobic interaction on the AuNP surfaces.[38] The lipophobicity (expressed as log *P*) values of the individual nitrogen bases were found to be −0.53, −0.46, −1.90, and −1.81 for the dA, dT, dC, and dG, respectively. The theoretical calculated data indicate that the dA and dT should be more hydrophobic than the dC and dG. The 3D sketch also illustrates that the lipophobicity of the oligonucleotides may play an important role in the AuNP adsorption as a result of the nitrogen bases surrounding the oligonucleotide, whereas the negative charged phosphodiester bonding is located in the center of the molecule (Figure S2, Supporting Information). Although the dT_{20} is more lipophobic than the dA_{20}, the dA_{20} exhibited a better protective ability (red) than the dT_{20} (pink). Comparing the end view of the 3D sketches of dA_{20} and dT_{20} (Figure 4), the nitrogen base of the dA_{20} exhibited a regular arrangement in a specific direction and formed a planarlike structure. The planarlike structure of the dA_{20} attached onto the AuNPs along one plane of the molecule and may leads to stronger adsorption than that of the dT_{20}. Therefore, Figure 2c has shown the similar lipophobicity but differing color between the dA_{20}-AuNPs and the dT_{20}-AuNPs. However, more experiments are needed for further demonstration. This result not only demonstrated that the negatively charged DNA could serve as a protective agent for the AuNPs but also showed that the protective ability of each oligonucleotide for the AuNPs is different. The colors of the oligonucleotide-AuNPs (Figure 2c) could be divided into two groups: reddish (dA_{20}-AuNPs, dT_{20}-AuNPs) and bluish (dC_{20}-AuNPs, dG_{20}-AuNPs). The nanosensing of oligonucleotides with four nitrogen bases was first demonstrated by dividing the bases into two subgroups (A/T and C/G) using the representative colors that correspond to Watson−Crick base pairing. These color groups can be used to discriminate between the dA and the dC in double-stranded, complementary DNA because the PCR products perfectly correspond to the Watson−Crick base pairings: if more dA (or dT) than dC (or dG) is contained in the amplicons, then the base divergence may be differentiated by a color reading of the

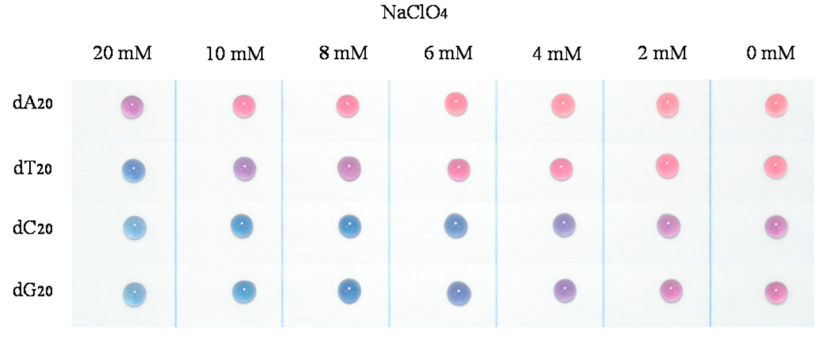

Figure 3. Effect of sodium perchlorate on the AuNP aggregation in the presence of oligonucleotides and a TA buffer (4 mM, pH 8.0). The sodium perchlorate can increase the ionic strength and enhance the aggregation of the AuNPs. Therefore, in this work, we used 10 mM sodium perchlorate to enhance the color difference between dA_{20}, dT_{20} and dC_{20}, dG_{20}. Other experimental conditions were the same as Figure 2c.

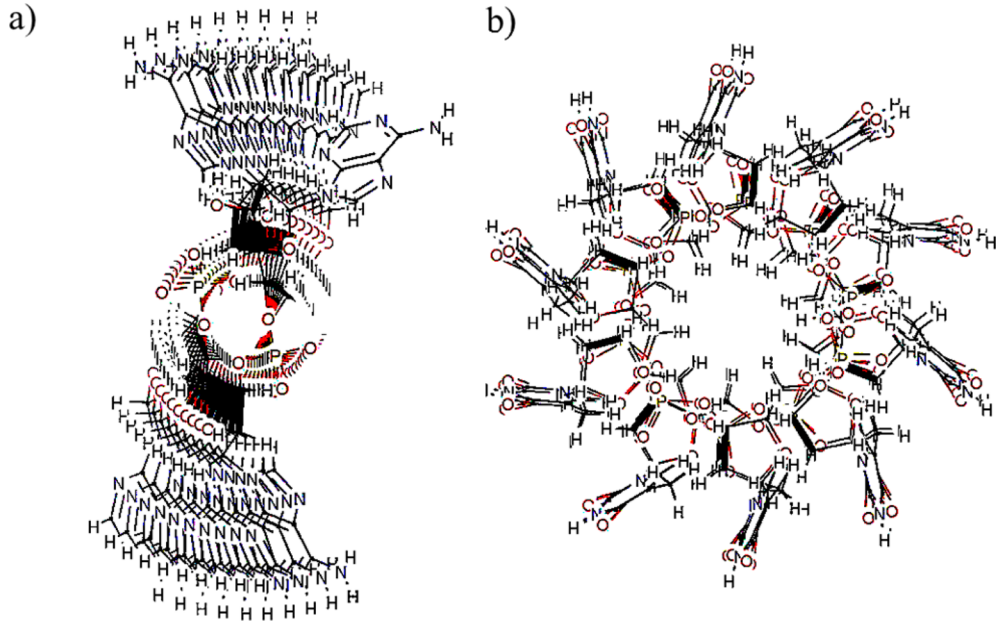

Figure 4. Computer simulated three-dimensional structure of the oligonucleotide with end view for dA_{20} (a) and dT_{20} (b). The space distribution of the phosphodiester bond, ribose, and nitrogen base of dA_{20} and dT_{20} can be observed clearly from the side view of the structure and is available in the Supporting Information (Figure S2).

nanosensor due to the enhanced adsorption of the DNA (dA and dT) onto the AuNPs.

Nanosensing of DNA Methylation from PCR Products. In this study, the proposed method was examined regardless of whether the nanosensor could discern the methylated DNA heterogeneity of cancer cell lines. The HK-1 cells were treated with 5-aza-2′-deoxycytodine for 1−5 days followed by DNA extraction and the nanosensing procedure (Figure 5a). After completion of the sensing procedure, the color of the cell lines changed from blue to violet and finally to pink (after treatment for 5 days). The amplified DNA region of the HK-1 cells (control) is expected to be highly methylated and thus has a high G/C content within the PCR amplicons. However, the methylation level of the genomic DNA decreased when the cells were treated with 5-aza-2′-deoxycytidine for up to 5 days. The amplicons should have contained more dT and its complementary dA than dC or dG, as indicated by the pink color shown in Figure 5a. It should be noted that the amplicons can be as long as 342 bp. Unlike the synthetic oligonucleotides (Figure 2c), this DNA sample was double stranded, and the composition of PCR amplicons was more complex than that of the oligonucleotides with consistent nitrogen bases. Despite this observation, our data demonstrates that the AuNPs nanosensor is useful for the rapid screening of DNA in the presence of high and/or low methylation states (Figure 5a). A color change from pink to blue was found when 12 cancer cell lines were screened using this nanosensor. With the nasopharyngeal carcinoma (NPC) cells (C666-1, HK-1, TW04, TW02) the AuNP color change from deep blue to violet indicated the highest methylation level (Figure 5b). This result is not surprising because the genomic region chosen for amplification is hyper-methylated in NPC.[34] In comparison, other cancer cell lines displayed a moderate or low methylation level. The cells other than the NPC cells could not be differentiated by observing them with the naked eye due to their similar colors; however, these samples could be easily differentiated via UV−visible spectrophotometry (Figure 5c). The samples were then transferred to a UV−visible spectrophotometer to obtain the absorption spectrum of the AuNPs. Distinguishing the cancer types becomes simple, as using the ratio of absorbances ($\lambda_{650}/\lambda_{518}$) facilitates discrimination of the cancer types. In Figure 5c, HK-1 has the highest methylation level of the four NPC cell lines; TW02 and TW04 present slightly lower methylation levels than HK-1. However, the methylation levels of the three cell lines, as determined by

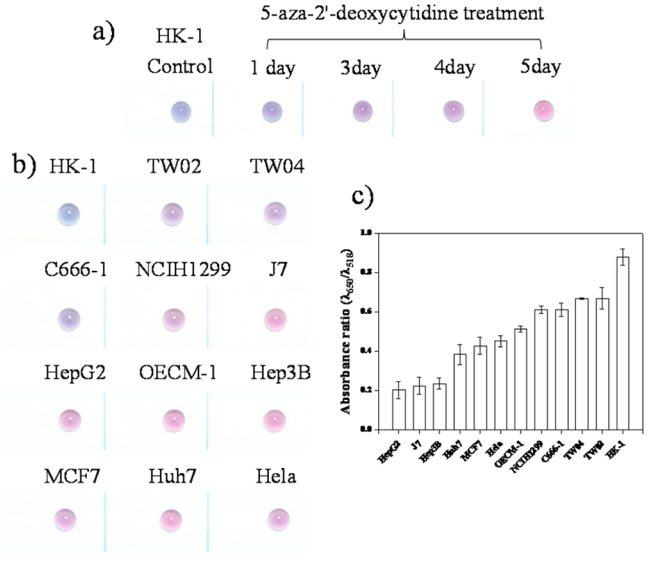

Figure 5. Determination of DNA methylation in cancer cells using an AuNP nanosensor. (a) Samples from the cultured HK-1 cells treated with 5-aza-2′-deoxycytidine for 1−5 days. (b) Nanosensing of the DNA methylation for 12 cancer cell lines. (c) Column plot of the $\lambda_{650}/\lambda_{518}$ ratio for each cell line. The λ_{518} is the surface plasmon absorption of the AuNPs, and the λ_{650} indicates the AuNPs aggregation that results from the surface plasmon shift. The experiments were performed in triplicate to obtain the means and standard deviations. Other experimental conditions were the same as Figure 2c.

capillary electrophoresis with laser-induced fluorescence, are all similar (>99%). One reasonable explanation for this result is that the three cell lines have high heterogeneity in their DNA methylation. A special case, C666-1, which was an NPC cell with the Epstein−Barr virus genome inserted into the genome of C666-1, exhibited less methylation than the other NPC cells, which also corresponded to the electropherograms that were obtained from COBRA.[34] In addition to CE-LIF, the nanosensor for DNA methylation was also compared with MS-HRM. The MS-HRM is a real-time PCR-based technique, and it determines the DNA methylation in the easiest manner possible. The bisulfite-treated genomic DNA is amplified in a real-time PCR machine with a fluorescent saturating dye[36] followed by melting curve analysis. If methylation occurs on genomic DNA, the difference of that T/C quantity of sense, single-stranded DNA may cause a change in the melting temperature (T_m), altering the differential curve of fluorescence intensity. That is, the more methylated cytosine that is present results in a higher T_m because of greater number of hydrogen bonds that formed between cytosine and guanine. Compared to the MS-HRM data of the four NPC samples (Figure 6), a

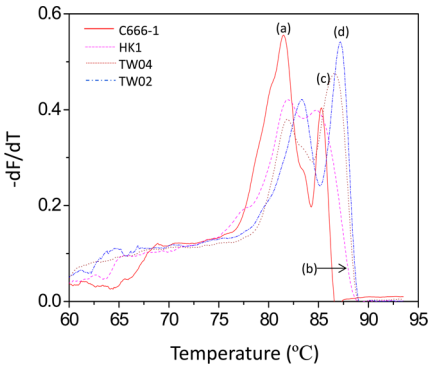

Figure 6. High-resolution melting curve of amplified PCR products for four NPC cells (a) C666-1, (b) HK-1, (c) TW04, and (d) TW02. The samples have been comfirmed by combined bisulfite-restriction assay with capillary electrophoresis. The methylation levels of C666-1, HK-1, TW04, and TW02, were 75.1%, 99.0%, 99.4%, and 99.8%, respectively.[2]

similar tendency was also observed. The C666-1 cells (Figure 6a) have smallest T_m (about 77−87 °C), which indicates the lowest methylation level among the four cells as a result of more A/T base pairing. By contrast, however, the greatest G/C content of the TW02 cells displayed the highest T_m in the MS-HRM curve (Figure 6d). The shown data demonstrates that the MS-HRM analysis is consistent with COBRA, but the slight difference (<1%) between TW02, TW04, and HK-1 cannot be discriminated exactly by nanosensors. However, a previous study indicated that the MS-HRM was affected not only by the properties of DNA (the methylation level and the heterogeneity of methylation) but also by the characteristics of the dye, which may generate an uncertainty of T_m because of the fluorescent dye preferential binding to GC-rich sequences.[42] Therefore, the AuNPs nanosensor serves as an economical and convenient assay for the screening of DNA methylation and should be enough for most epigenetic applications.

CONCLUSIONS

In summary, this study found that AuNPs could be used to differentiate among DNA with four different nitrogen bases. These findings support the proposal of a method for determining DNA methylation using a colorimetric nanosensor. The genomic DNA that underwent bisulfite conversion, PCR amplification, and the DNA methylation could be evaluated directly using naked-eye observations. Moreover, the heterogeneity of the DNA methylation within a single type of cancer cell could be determined using the AuNPs nanosensor. On the other hand, this proposed nanosensor without any conjugated target specific ligand such as DNA or proteins leads to a nanosensor easy to manufacture for nanosensing. The COBRA technique is the more traditional technique for quantitative analysis of DNA methylation based on the change of fluorescence intensity of digested PCR products.[8] In addition to quantitative analysis, the restriction endonuclease-based technique also provides more precise information for the determination of the heterogeneity of DNA methylation.[9] However, COBRA-CE only evaluates a few CpG sites within this amplicons because of the limited available restriction endonuclease. Compared with MS-HRM analysis,[10] this proposed method did not require instrumentation or a special saturating dye[36] and the amplicons used in this study could be as long as 342 bp. Therefore, we believe the proposed DNA methylation nanosensor not only may benefit researchers studying epigenetics but also may promote the development of epigenetics-based biomarkers.[7]

ASSOCIATED CONTENT

Supporting Information

The mercaptopropionic acid effect on the discrimination power of the nanosensor for oligonucleotides and the computer simulated three-dimensional structure of the oligonucleotide. This material is available free of charge via the Internet at http://pubs.acs.org.

AUTHOR INFORMATION

Corresponding Author

*P.-L. Chang. E-mail: poling@thu.edu.tw. Address: No. 1727, Sec. 4, Taiwan Boulevard, Xitun District, Taichung 40704, Taiwan.

Notes

The authors declare no competing financial interest.

ACKNOWLEDGMENTS

This work was supported by grants-in-aid from the National Science Council, Taiwan, (NSC100-2113-M-029-008-MY2, 102-2113-M-029-002-MY2). P.-L. Chang also thanks Prof. Y.-S. Chang, Prof. S.-J. Chen, and Prof. H.-C. Chen for kindly providing the cancer cells used in this work (Molecular Medicine Research Center, Chang Gung University).

REFERENCES

(1) Laird, P. W.; Jaenisch, R. *Annu. Rev. Genet.* **1996**, *30*, 441−464.
(2) Geiman, T. M.; Muegge, K. *Mol. Reprod. Dev.* **2010**, *77*, 105−113.
(3) Esteller, M. *Adv. Exp. Med. Biol.* **2003**, *532*, 39−49.
(4) Kondo, Y.; Issa, J. P. *Expert Rev. Mol. Med.* **2010**, *12*, e23.
(5) Richardson, B. *Ageing Res. Rev.* **2003**, *2*, 245−261.
(6) Esteller, M. *Curr. Opin. Oncol.* **2005**, *17*, 55−60.
(7) Levenson, V. V. *Expert Rev. Mol. Diagn.* **2010**, *10*, 481−488.
(8) Goedecke, S.; Schlosser, S.; Muhlisch, J.; Hempel, G.; Fruhwald, M. C.; Wunsch, B. *Electrophoresis* **2009**, *30*, 1412−1417.
(9) Chen, H. C.; Chang, Y. S.; Chen, S. J.; Chang, P. L. *J. Chromatogr. A* **2012**, *1230*, 123−129.
(10) Wojdacz, T. K.; Dobrovic, A. *Nucleic Acids Res.* **2007**, *35*, e41.

(11) Wong, E. M.; Dobrovic, A. *Methods Mol. Biol.* **2011**, *687*, 207−217.
(12) Tost, J.; Gut, I. G. *Nat. Protoc.* **2007**, *2*, 2265−2275.
(13) Flusberg, B. A.; Webster, D. R.; Lee, J. H.; Travers, K. J.; Olivares, E. C.; Clark, T. A.; Korlach, J.; Turner, S. W. *Nat. Methods* **2010**, *7*, 461−465.
(14) Schmitz, O. J.; Worth, C. C.; Stach, D.; Wiessler, M. *Angew. Chem., Int. Ed.* **2002**, *41*, 445−448.
(15) Wang, X.; Song, Y.; Song, M.; Wang, Z.; Li, T.; Wang, H. *Anal. Chem. (Washington, DC, U. S.)* **2009**, *81*, 7885−7891.
(16) Wang, X.; Suo, Y.; Yin, R.; Shen, H.; Wang, H. *J. Chromatogr. B: Anal. Technol. Biomed. Life Sci.* **2011**, *879*, 1647−1652.
(17) Xiong, Z.; Laird, P. W. *Nucleic Acids Res.* **1997**, *25*, 2532−2534.
(18) Wojdacz, T. K.; Moller, T. H.; Thestrup, B. B.; Kristensen, L. S.; Hansen, L. L. *Expert Rev. Mol. Diagn.* **2010**, *10*, 575−580.
(19) Kim, H. N.; Ren, W. X.; Kim, J. S.; Yoon, J. *Chem. Soc. Rev.* **2012**, *41*, 3210−3244.
(20) Vilela, D.; Gonzalez, M. C.; Escarpa, A. *Anal. Chim. Acta* **2012**, *751*, 24−43.
(21) Elghanian, R.; Storhoff, J. J.; Mucic, R. C.; Letsinger, R. L.; Mirkin, C. A. *Science* **1997**, *277*, 1078−1081.
(22) Huang, C.-C.; Yang, Z.; Lee, K.-H.; Chang, H.-T. *Angew. Chem., Int. Ed.* **2007**, *46*, 6824−6828.
(23) Miyake, Y.; Togashi, H.; Tashiro, M.; Yamaguchi, H.; Oda, S.; Kudo, M.; Tanaka, Y.; Kondo, Y.; Sawa, R.; Fujimoto, T.; Machinami, T.; Ono, A. *J. Am. Chem. Soc.* **2006**, *128*, 2172−2173.
(24) Li, M.; Wang, Q.; Shi, X.; Hornak, L. A.; Wu, N. *Anal. Chem.* **2011**, *83*, 7061−7065.
(25) Ferhan, A. R.; Guo, L.; Zhou, X.; Chen, P.; Hong, S.; Kim, D. H. *Anal. Chem.* **2013**, *85*, 4094−4099.
(26) Liu, C.-Y.; Tseng, W.-L. *Chem. Commun.* **2011**, *47*, 2550−2552.
(27) Wang, J.; Wang, L.; Liu, X.; Liang, Z.; Song, S.; Li, W.; Li, G.; Fan, C. *Adv. Mater.* **2007**, *19*, 3943−3946.
(28) Zhu, X.; Yang, Q.; Huang, J.; Suzuki, I.; Li, G. *J. Nanosci. Nanotechnol.* **2008**, *8*, 353−357.
(29) Xu, Y.; Wang, J.; Cao, Y.; Li, G. *Analyst* **2011**, *136*, 2044−2046.
(30) Zhu, X.; Liu, Y.; Yang, J.; Liang, Z.; Li, G. *Biosens. Bioelectron.* **2010**, *25*, 2135−2139.
(31) Liu, T.; Zhao, J.; Zhang, D.; Li, G. *Anal. Chem.* **2010**, *82*, 229−233.
(32) Wang, J.; Zhu, Z.; Ma, H. *Anal. Chem.* **2013**, *85*, 2096−2101.
(33) Liu, Y.-C.; Chang, H.-T.; Chiang, C.-K.; Huang, C.-C. *ACS Appl. Mater. Interfaces* **2012**, *4*, 5241−5248.
(34) Chen, H.-C.; Chang, Y.-S.; Chen, S.-J.; Chang, P.-L. *J. Chromatogr., A* **2012**, *1230*, 123−129.
(35) Kent, W. J.; Sugnet, C. W.; Furey, T. S.; Roskin, K. M.; Pringle, T. H.; Zahler, A. M.; Haussler, D. *Genome Res.* **2002**, *12*, 996−1006.
(36) Monis, P. T.; Giglio, S.; Saint, C. P. *Anal. Biochem.* **2005**, *340*, 24−34.
(37) Clark, S. J.; Harrison, J.; Paul, C. L.; Frommer, M. *Nucleic Acids Res.* **1994**, *22*, 2990−2997.
(38) Liu, J. *Phys. Chem. Chem. Phys.* **2012**, *14*, 10485−10496.
(39) Li, D.; Wieckowska, A.; Willner, I. *Angew. Chem., Int. Ed.* **2008**, *47*, 3927−3931.
(40) Kumar, A.; Mandal, S.; Pasricha, R.; Mandale, A. B.; Sastry, M. *Langmuir* **2003**, *19*, 6277−6282.
(41) Li, H.; Rothberg, L. *Proc. Natl. Acad. Sci. U. S. A.* **2004**, *101*, 14036−14039.
(42) Gudnason, H.; Dufva, M.; Bang, D. D.; Wolff, A. *Nucleic Acids Res.* **2007**, *35*, e127.